THE JOURNAL OF PHYSICAL CHEMISTRY Letters

LETTER

pubs.acs.org/JPCL

Anisotropic Picosecond X-ray Solution Scattering from Photoselectively Aligned Protein Molecules

Jeongho Kim,[†] Kyung Hwan Kim,[†] Jong Goo Kim, Tae Wu Kim, Youngmin Kim, and Hyotcherl Ihee*

Center for Time-Resolved Diffraction, Department of Chemistry, Graduate School of Nanoscience & Technology (WCU), KAIST, Daejeon, Republic of Korea

ABSTRACT: Anisotropic X-ray scattering patterns of transiently aligned protein molecules in solution are measured by using pump−probe X-ray solution scattering. When a linearly polarized laser pulse interacts with an ensemble of molecules, the population of excited molecules is created with their transition dipoles preferentially aligned along the laser polarization direction. We measured the X-ray scattering from the myoglobin protein molecules excited by a linearly polarized, short laser pulse and obtained anisotropic scattering patterns on a 100 ps time scale. An anisotropic scattering pattern contains higher structural information content than a typical isotropic pattern available from randomly oriented molecules. In addition, multiple independent diffraction patterns measured by using various laser polarization orientations will give a substantially increased amount of structural information compared with that from a single isotropic pattern. By monitoring the temporal change of the anisotropic scattering pattern from 100 ps to 1 μs, we observed the orientational dynamics of photogenerated myoglobin with the rotational diffusion time of ∼15 ns.

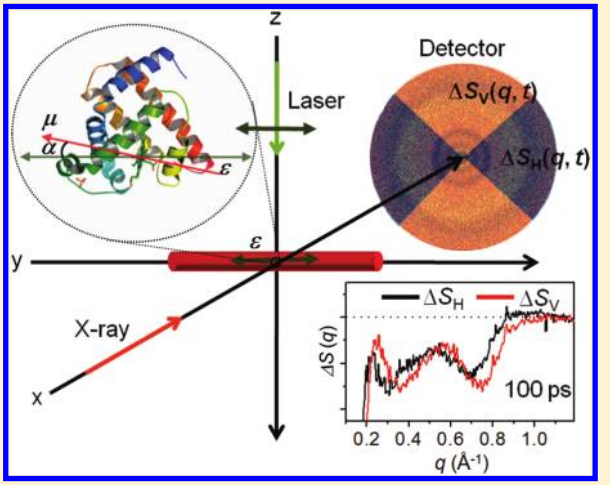

SECTION: Kinetics, Spectroscopy

Time-resolved X-ray solution scattering (liquidography) offers a means of directly accessing the transient molecular structure in the solution phase, for example, the time dependence of bond lengths and angles. Structural dynamics of various molecular systems in solution including diatomic molecules, haloalkanes, organometallic complexes, protein molecules, and nanoparticles have been elucidated using this technique.[1−15] Due to the lack of long-range order and random orientation of molecules in solution, a solution scattering pattern generally exhibits an isotropic, smooth oscillation profile, containing much less information content compared with diffraction patterns from crystalline samples. Enhancing information content would allow extraction of more accurate structures and dynamics. As one of the first steps toward this goal, here, we investigate the possibility of increasing the information content by manipulating the polarization orientation of the pump laser pulse relative to the X-ray propagation direction. As a result, the excited molecules are photoselectively aligned and generate anisotropic X-ray scattering patterns.

To some extent, this approach is similar to time domain spectroscopy using polarized light, which has been a powerful tool for selectively probing molecular orientational dynamics in isotropic media.[16−20] One of the most representative polarization spectroscopic techniques is pump−probe transient anisotropy, which can measure the depolarization rate. When a linearly polarized laser pulse interacts with an ensemble of molecules, the population of excited molecules is created with their transition dipoles preferentially aligned along the laser polarization direction. By using another linearly polarized light propagating in the same direction as the first laser beam as a probe, the evolution of a transition dipole direction over time can be probed in real time. The transient anisotropy has been mainly used for measuring rotational diffusion of molecules[21,22] as well as energy transfer dynamics in multichromophore systems such as conjugated polymers[23,24] and photosynthetic light-harvesting complexes.[25,26] In addition, important insight has been gained from polarization anisotropy studies of aqueous systems in the infrared region.[27−29]

With the advance in time-resolved diffraction techniques, the potential of probing the molecular orientational dynamics using electron diffraction has been investigated.[30−33] Especially, when applied to time-resolved diffraction techniques, it has been anticipated that linearly polarized excitation can help to characterize the molecular structure and dynamics more clearly because it has the effect of freezing the molecular orientation along the polarization direction. Conversely, the anisotropy effect manifested in the diffraction pattern could mislead the interpretation of the diffraction pattern. Therefore, more careful treatment is needed in the analysis of the anisotropic diffraction pattern.

Received: November 5, 2010
Accepted: January 24, 2011

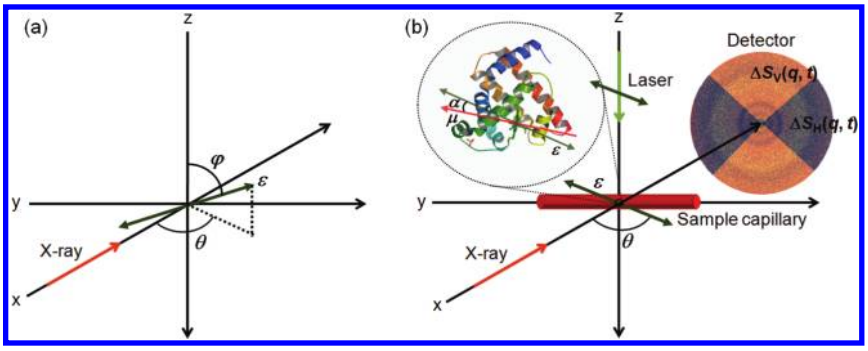

Figure 1. Concept of X-ray scattering from selectively aligned protein molecules. (a) With respect to the X-ray propagation direction (x-axis), the polarization (ε) of the laser pulse can have any orientation defined by θ and φ in spherical coordinates, where $0 \le \theta \le \pi/2$ and $0 \le \varphi \le \pi/2$. (b) In our experiment, the laser light with linear polarization was sent along the z-direction (setting $\varphi = \pi/2$), and only the θ value was varied between 0 and $\pi/2$. The orientation of the transition dipole (μ) of a molecule is described by the angle α with respect to the laser polarization (ε). The red cylinder represents a capillary containing protein solution. With the interaction of molecules in an ensemble with a linearly polarized laser pulse, the population of excited molecules is created with their transition dipoles preferentially aligned along the laser polarization direction in proportion to $\cos^2 \alpha$. We used linearly polarized light with $\theta = 0$ (i.e., parallel to the X-ray propagation) and $\theta = \pi/2$ (i.e., perpendicular to the X-ray propagation) and the circularly polarized light (θ varies from 0 to $\pi/2$) as the laser excitation source. Two-dimensional scattering patterns from transiently aligned molecules were obtained, and the anisotropy of the 2D pattern was examined by comparing the 1D curves of the vertical (ΔS_V) and horizontal (ΔS_H) cuts of the pattern.

In contrast to the gas-phase ultrafast electron diffraction technique, of which the time resolution reaches down to a few picoseconds, time-resolved X-ray diffraction (scattering) using third-generation synchrotrons currently has a time resolution of only ~100 ps. Thus, the anisotropy effect on the X-ray diffraction pattern has not been seriously considered so far because the rotational diffusion of small molecules commonly occurs on a much shorter time scale than 100 ps. However, with the advent of femtosecond X-ray pulses from the X-ray free-electron laser (XFEL), consideration of the anisotropic effect in the X-ray diffraction pattern will become increasingly important in the future experiments using femtosecond X-ray pulses.[34]

In this paper, we report for the first time the anisotropic X-ray scattering patterns from transiently aligned protein molecules in solution. To generate anisotropic scattering patterns that can be observed with 100 ps time resolution available from third-generation synchrotrons, we used a macromolecule, namely, myoglobin (Mb), instead of small molecules. Because Mb has much larger size than small molecules, its transient anisotropy lasts over ~10 ns.[35−37] Therefore, it is a relevant system for examining the effect of linearly polarized excitation on the X-ray scattering pattern using 100 ps X-ray solution scattering. Mb, a prototypical model system for studying protein structural dynamics, is a heme protein that carries ligands such as O_2, CO, and NO in oxygen transport in muscles. In its ligated form with a CO ligand, the ligand forms a covalent bond with Fe^{2+} of the heme group and is photolyzed by visible light on the subpicosecond time scale.[38,39] In our experiment, the excited Mb molecules are selectively aligned by photodissociation of a CO ligand from the metal ion of the heme group in the carboxymyoglobin (MbCO) using a linearly (or circularly) polarized picosecond laser pulse. Complex structural kinetics of Mb with multiexponential decays from 100 ps to 1 μs have been recently elucidated using X-ray solution scattering.[40,41]

The geometry of our experimental setup is shown in Figure 1. We consider a laser polarization orientation (ε) with the X-ray propagating along the x-axis in a laboratory-fixed reference frame. An arbitrary laser polarization orientation can be described by a combination of spherical coordinates θ and φ in the range of $0 \le \theta \le \pi/2$ and $0 \le \varphi \le \pi/2$. When a linearly polarized laser pulse interacts with an ensemble of molecules, the population of excited molecules is created with their transition dipoles preferentially aligned along the laser polarization direction in proportion to $\cos^2 \alpha$, where α is an angle between the transition dipole (μ) and the laser polarization (ε). In our experiment, the laser pulse with linear polarization was sent from the top along the z-axis, thereby fixing φ at $\pi/2$, and only the θ value was adjusted between 0 and $\pi/2$. The two-dimensional (2D) diffraction patterns obtained from transiently aligned molecules using various polarization orientations in this range form a basis set consisting of unique, linearly independent 2D diffraction patterns. Because multiple independent diffraction patterns can be obtained in this scheme, contrary to a single isotropic pattern typically obtained from randomly oriented molecules, the structural information content can be substantially increased. The 2D patterns obtained from any polarization orientations (any θ and φ) can be reverted to one of these basis 2D patterns via rotation around the x-axis. In particular, we examined the polarization effect using linearly polarized light with $\theta = 0$ (i.e., parallel to the X-ray propagation) and $\theta = \pi/2$ (i.e., perpendicular to the X-ray propagation) and the circularly polarized light (θ varies from 0 to $\pi/2$) as the laser excitation source. It should be noted that in polarization spectroscopy, the pump and probe pulses typically propagate in nearly the same direction as each other and the relative angle between the polarizations of two pulses is the key parameter for the observation of anisotropy. On the contrary, in our approach for anisotropic X-ray scattering, the polarization orientation of the pump laser pulse relative to the X-ray propagation direction is the relevant parameter. We also note that the probe X-ray itself is linearly polarized, and thus, the scattering pattern is already anisotropic due to this X-ray polarization, even if the sample is isotropic in molecular orientation. However, this does not increase the information content of the scattered signal because every molecule in the sample experiences the same X-ray polarization regardless of the molecular orientation. This kind of anisotropy due to the intrinsic X-ray polarization should be distinguished from the anisotropy induced by the laser polarization of the pump pulse discussed in this work.

To examine the laser polarization effect on the obtained scattering pattern, we first checked the 1D curves obtained from the cuts of the 2D scattering image along its horizontal and vertical directions $\Delta S_H(q,t)$ and $\Delta S_V(q,t)$, respectively, as shown

dx.doi.org/10.1021/jz101503r |J. Phys. Chem. Lett. 2011, 2, 350–356

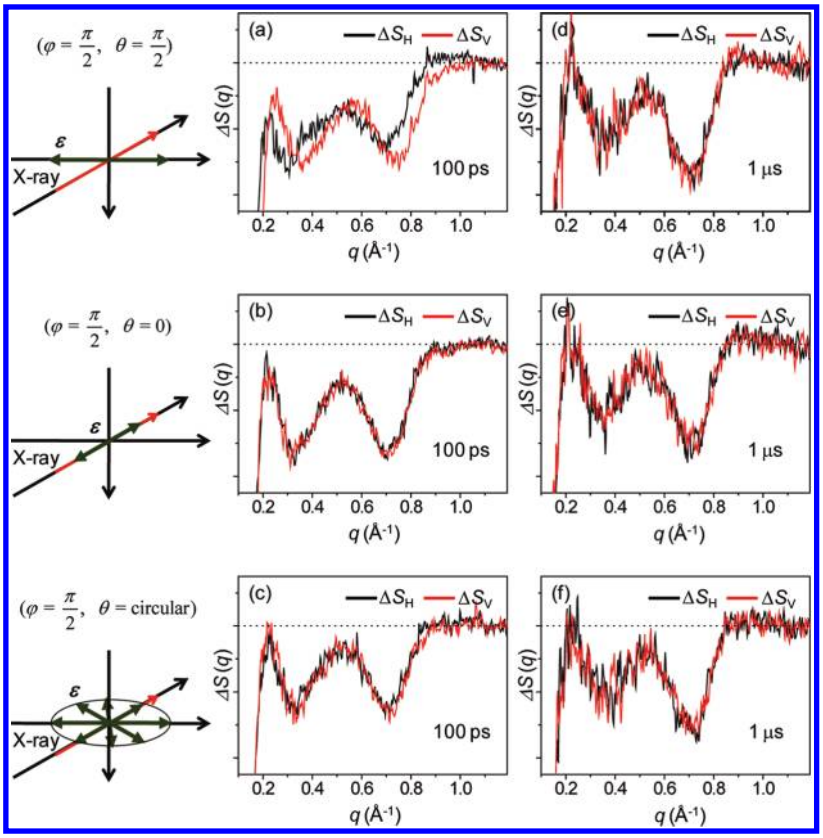

Figure 2. 1D scattering curves, $\Delta S_H(q,t)$ and $\Delta S_V(q,t)$, obtained from horizontal (black) and vertical (red) cuts of the 2D difference patterns of Mb measured at (a−c) 100 ps and (d−f) 1 μs time delays. The directions of linear laser polarization and X-ray propagation were adjusted to be (a, d) perpendicular ($\theta = \pi/2$) and (b, e) parallel ($\theta = 0$), or (c, f) circularly polarized light was used as the laser excitation source. Also, the orientations of the laser polarization and the X-ray propagation are schematically shown on the left.

in Figure 2. In Figure 2a, when the laser polarization is perpendicular to the direction of X-ray propagation, the difference between the horizontal and vertical cross sections can be clearly seen at a 100 ps time delay. As time goes on, the anisotropy in the scattering pattern decays and completely vanishes in the data at a 1 μs time delay. In contrast, in Figure 2b, when the laser polarization is parallel to the X-ray propagation direction, no distinct difference between the horizontal and vertical cuts is seen even at 100 ps. In this case, the lack of distinct anisotropy between the horizontal and vertical cuts can be ascribed to the experimental condition that the direction of laser polarization is identical to the X-ray propagation direction. Due to such experimental geometry, any anisotropy induced by linear laser polarization cannot be mapped out in the image plane of the 2D CCD detector, which is perpendicular to the direction of both laser polarization and X-ray propagation. However, the laser polarization still affects the scattering image in this geometry, and the effect will be manifested in the decay dynamics of the diffraction pattern over time, regardless of the lack of distinct anisotropy in a diffraction pattern measured at a certain time delay.

We also examined the polarization effect using circularly polarized excitation, as shown in Figure 2c. Because circularly polarized light can be described as a linear combination of two orthogonal linearly polarized lights with equal contribution, we can expect to see the anisotropy in the scattering pattern to some extent. As expected, the difference between the vertical and horizontal cuts can be seen in the data measured at a 100 ps time delay, although it is not as distinct as that in Figure 2a.

We also azimuthally averaged the entire 2D scattering patterns to obtain 1D scattering curves for the cases of perpendicular and parallel laser polarization−X-ray propagation geometries. The two 1D curves, $\Delta S_{\theta=\pi/2}(q,t)$ and $\Delta S_{\theta=0}(q,t)$, are compared in Figure 3a−c for three representative time delays (100 ps, 3.16 ns, and 1 μs). The difference between the scattering curves measured with the perpendicular and parallel polarizations of laser excitation is clearly seen at 100 ps, decreases at 3.16 ns, and completely vanishes at 1 μs. Here, it should be noted that the polarization-dependent alignment effect is still manifested in the 1D scattering curves obtained by azimuthally integrating the 2D patterns. The azimuthal integration averages the 2D diffraction pattern around the X-ray propagation direction, and therefore, it has the effect of destroying the anisotropy in the 2D diffraction pattern. However, despite the azimuthal integration, the spatial distributions of the photoselected molecules from the parallel and perpendicular excitations are still different even after the averaging around the X-ray propagation direction. Thus, the difference between the scattering signals measured with the parallel and perpendicular geometry of laser polarization and X-ray propagation is still distinct in the 1D scattering curves. To completely eliminate such residual anisotropy in the 1D curve obtained by azimuthal integration, circularly polarized light should be used as the excitation source. In fact, to remove this polarization effect, circularly polarized light is commonly used in the pump−probe X-ray solution scattering experiment for the samples with large size and slow rotational diffusion.

To follow the time evolution of the anisotropy manifested in the X-ray scattering pattern, at each time delay, we took the

dx.doi.org/10.1021/jz101503r |J. Phys. Chem. Lett. 2011, 2, 350–356

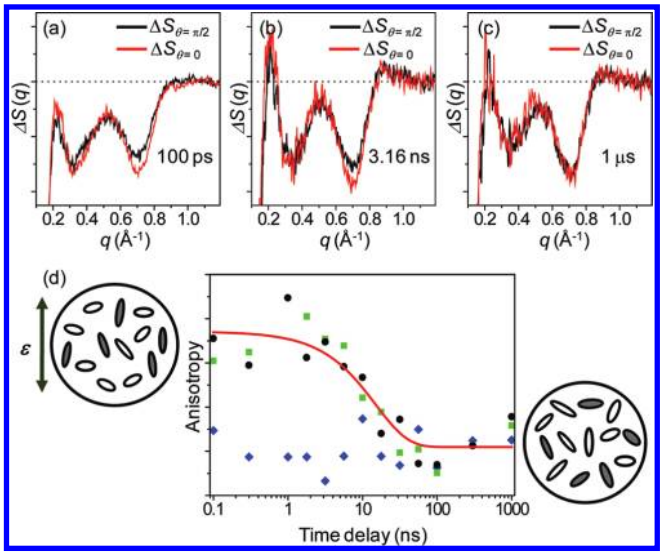

Figure 3. The polarization-dependent alignment effect survives even in the 1D scattering curves obtained by azimuthally integrating the 2D patterns. The 1D curves, $\Delta S_{\theta=\pi/2}(q,t)$ and $\Delta S_{\theta=0}(q,t)$, measured by using perpendicular (black) and parallel (red) geometries of the linear laser polarization and X-ray propagation direction are shown together at three representative time delays of (a) 100 ps, (b) 3.16 ns, and (c) 1 μs. The difference is clearly seen at 100 ps and decreases over time. (d) Time evolution of transient anisotropy obtained from the X-ray scattering curves. The difference between the parallel and perpendicular cases (black circles) reflects the degree of anisotropy (see eq 1) and thus can be used to follow the rotational diffusion of the protein molecules in solution. Also, the perpendicular case alone can be used to extract the anisotropy by taking the difference between the vertical and horizontal cross sections (green squares) (see eq 2), whereas the difference between the same cross sections does not show any anisotropy in the parallel case (blue diamonds). The red curve is a fit to the observed time-dependent anisotropy (black circles), and the decay time constants of both anisotropies, 15 ± 6 ns, match the rotational diffusion rate of the same protein obtained from other studies.

difference between the two scattering curves from the perpendicular and parallel cases and integrated it along the q-axis to define a measure of polarization anisotropy contained in the X-ray scattering patterns as follows

$$\text{Anisotropy}(t) = \frac{\sum_i |(\Delta S_{\theta=\pi/2}(q_i,t) - \Delta S_{\theta=0}(q_i,t))/\sqrt{\sigma^2_{\theta=\pi/2}(q_i,t)+\sigma^2_{\theta=0}(q_i,t)}|}{\sum_i |\Delta S_{\theta=\pi/2}(q_i,t)| + \sum_i |\Delta S_{\theta=0}(q_i,t)|} \quad (1)$$

where $\sigma(q_i,t)$ means the standard deviation of the $\Delta S(q_i,t)$. The time evolution of the anisotropy is plotted in Figure 3d. Also, the perpendicular case alone can be used to extract the anisotropy by taking the difference between the 1D curves from the vertical and horizontal cross sections as follows

$$\text{Anisotropy}(t) = \frac{\sum_i |(\Delta S_{\mathrm{H}}(q_i,t) - \Delta S_{\mathrm{V}}(q_i,t))/\sqrt{\sigma^2_{\mathrm{H}}(q_i,t)+\sigma^2_{\mathrm{V}}(q_i,t)}|}{\sum_i |\Delta S_{\mathrm{H}}(q_i,t)| + \sum_i |\Delta S_{\mathrm{V}}(q_i,t)|} \quad (2)$$

The observed anisotropy decay of aligned Mb molecules can be fitted by an exponential of the ~15 ns time constant, which agrees well with the rotational diffusion time measured by NMR (10 ns in ref 35 and 15−20 ns in ref 36) and the value predicted by the Stokes−Einstein equation (11 ns). Thus, the transient anisotropy measured by picosecond X-ray solution scattering is relevant for measuring the orientational dynamics of the protein molecules. Also, it should be noted that the rotational diffusion time measured in our work is for the Mb molecules generated by photolysis, whereas those measured by NMR are for unexcited Mb molecules. Therefore, our technique serves as a useful method that can measure the rotational diffusion time of photogenerated protein species.

The anisotropic X-ray scattering pattern observed in this work can be easily explained theoretically. For this purpose, we simulated 2D difference X-ray scattering patterns from the hypothetical photoinduced structural change of iodine (I_2) in the gas phase as a model system. For this reaction, we took into account the fact that the probability of initial excitation is governed by the $\cos^2 \alpha$ relationship, where α is the angle between the laser polarization and the transition dipole of the iodine molecule. Figure 4a and b shows the simulated difference scattering patterns for the perpendicular and parallel laser polarization−X-ray propagation cases, respectively. Clearly, the 2D difference scattering image for the perpendicular case (Figure 4a) shows an anisotropic pattern, while that for the parallel case (Figure 4b) is isotropic. As in Figure 2, we also show the 1D curves, $\Delta S_{\mathrm{H}}(q)$ and $\Delta S_{\mathrm{V}}(q)$, obtained from the cuts of the 2D scattering image along its horizontal and vertical directions, respectively. The difference between $\Delta S_{\mathrm{H}}(q)$ and $\Delta S_{\mathrm{V}}(q)$ is clearly seen in the perpendicular case (Figure 4a), which corresponds to Figure 2a. In contrast, $\Delta S_{\mathrm{H}}(q)$ and $\Delta S_{\mathrm{V}}(q)$ are identical in the parallel case (Figure 4b), which corresponds to Figure 2b. In Figure 4c, we also compare azimuthally averaged 1D scattering curves, $\Delta S_{\theta=\pi/2}(q)$ and $\Delta S_{\theta=0}(q)$, for the cases of perpendicular and parallel laser polarization−X-ray geometries, respectively. As in Figure 3a, it can be clearly seen that $\Delta S_{\theta=\pi/2}(q)$ and $\Delta S_{\theta=0}(q)$ are different.

In this work, from picosecond X-ray solution scattering using linearly polarized light, we obtained anisotropic scattering patterns of transiently aligned protein molecules for the first time. Because multiple independent diffraction patterns can be measured by using various laser polarization orientations relative to the X-ray propagation direction, a substantially increased amount of structural information can be obtained than from a single isotropic pattern typically available from randomly oriented molecules. Thus, if the anisotropic 2D diffraction patterns obtained from protein molecules of transiently fixed orientation can be analyzed in more detail with the development of advanced structural analysis tools, the transient structures of Mb associated with the photoinduced structural changes will be determined more accurately. In addition, by monitoring the time-dependent change of the anisotropic patterns, we extracted the time scale of the orientational dynamics of the protein molecule, which reflects the rotational diffusion time of photogenerated protein species. In the near future, with the development of femtosecond X-ray scattering experiments and appropriate theoretical tools to analyze the anisotropic scattering pattern, we expect that the molecular structure and dynamics will be determined more accurately, aided by the transient alignment using linearly polarized laser excitation.

EXPERIMENTAL SECTION

Time-resolved X-ray solution scattering data were measured at the 14IDB BioCARS beamline at the Advanced Photon Source

dx.doi.org/10.1021/jz101503r |J. Phys. Chem. Lett. 2011, 2, 350–356

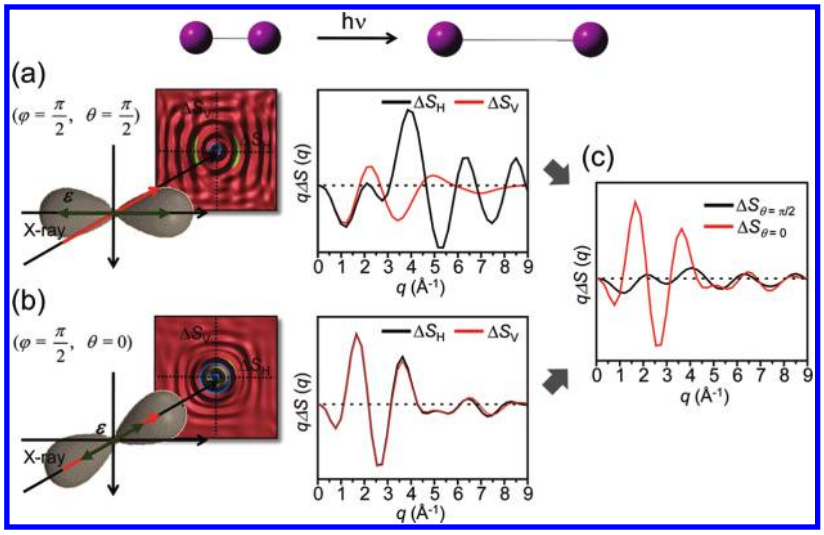

Figure 4. Theoretically calculated difference scattering patterns from a hypothetical photoinduced structural change of iodine (I_2) when using (a) perpendicular and (b) parallel geometries of the laser polarization and X-ray propagation direction. Due to the interaction with the laser electric field of linear polarization, the iodine molecules are excited following the $\cos^2 \alpha$ excitation probability. As a result, the spatial distribution of the excited population takes a dumbbell shape lying along the polarization direction. The 1D difference scattering curves correspond to the horizontal (ΔS_H) and vertical (ΔS_V) cuts of the calculated 2D difference scattering image. The difference between $\Delta S_H(q,t)$ and $\Delta S_V(q,t)$ is clearly seen in the case of the perpendicular case, while there is no difference between the two curves in the parallel case. (c) The 1D curves, $\Delta S_{\theta=\pi/2}$ and $\Delta S_{\theta=0}$, were obtained by azimuthally integrating the entire 2D images in the perpendicular (black) and parallel (red) geometries of the linear laser polarization and X-ray propagation direction. It can be clearly seen that the two curves are different. We note that the *y*-axis scale of the plot in (a) is three times larger than the ones in (b) and (c).

while the storage ring was operated in the standard operating top-up mode at 7 GeV. The usual experimental protocol[10,42] was followed. Specifically, equine heart MbCO solution (8 mM, pH 7.0, 0.1 M sodium phosphate) was excited by a ~30-ps-long laser pulse at 532 nm to initiate the CO photodissociation, and a ~100-ps-long single X-ray pulse was used as a probe to follow the progress of the reaction. The laser polarization was controlled by using a Berek compensator. A laser pulse of ~60 μJ energy was focused onto a spot of 0.65 mm × 0.16 mm size at the sample position, yielding an energy fluence of 0.6 mJ/mm^2. The sample was contained in a sealed quartz capillary of 1 mm diameter and maintained at 25 °C with a cold nitrogen stream (Oxford Cryostream). The laser and X-ray beams were crossed at the sample in a perpendicular geometry, as shown in Figure 1. The X-ray pulses scattered by the sample were recorded by a 2D MarCCD CCD detector as a function of the time delay between the laser and X-ray pulses. To attain enough signal-to-noise ratio, ~10 images were acquired at each time delay. To avoid radiation damage and provide a fresh sample for each pair of X-ray and laser pulses, the capillary containing the sample was translated by 0.2 mm after each probe pulse along its long axis over a 20 mm range. The laser-off images were acquired with laser pulses arriving 5 μs earlier than the X-ray pulse in order to probe the ground state while assuring the same average temperature of the solution. These laser-off images were used to compute the time-resolved X-ray scattering differences. The data were measured at time delays spread evenly in the logarithmic time scale and are as follows: −5 μs, 100 ps, 300 ps, 1 ns, 1.78 ns, 3.16 ns, 5.62 ns, 10 ns, 17.8 ns, 31.6 ns, 56.2 ns, 100 ns, 300 ns, 1 μs, and 30 ms.

For the simulation of hypothetical photoinduced structural change of iodine (I_2) in the gas phase, 30 000 randomly orientated iodine molecules were considered. The molecules become excited following the excitation probability of $\cos^2 \alpha$, where α is the angle between the laser polarization and the transition dipole of the iodine molecule. Once they are excited, it is assumed that the iodine molecule dissociates and the I−I distance changes from 2.67 to 4.00 Å. The 2D scattering image for the photoexcited sample was calculated by adding the 2D scattering images of the 30 000 molecules that can have either 4 (if excited) or 2.67 Å distance (if not excited). The 2D scattering image for the ground-state sample prior to photoexcitation was calculated by adding the 2D scattering images of the 30 000 molecules that have only 2.67 Å distance. Then, the difference was taken between the two images to give the difference 2D scattering pattern. The 1D scattering curves were calculated by azimuthally integrating the difference 2D scattering patterns. These calculations were repeated for perpendicular and parallel laser polarization−X-ray propagation geometries.

AUTHOR INFORMATION

Corresponding Author

*E-mail: hyotcherl.ihee@kaist.ac.kr.

Author Contributions

†These authors contributed equally to this work.

ACKNOWLEDGMENT

We acknowledge the BioCARS staff for discussions and experimental assistance. This work was supported by the Creative Research Initiatives (Center for Time-Resolved Diffraction) of MEST/NRF. Use of the BioCARS Sector 14 was supported by NIH (RR007707). J.K. and Y.K. acknowledge the support from the WCU program (R31-2008-000-10071-0).

REFERENCES

(1) Ihee, H. Visualizing Solution-Phase Reaction Dynamics with Time-Resolved X-ray Liquidography. *Acc. Chem. Res.* **2009**, *42*, 356–366.

(2) Kim, T. K.; Lee, J. H.; Wulff, M.; Kong, Q.; Ihee, H. Spatiotemporal Kinetics in Solution Studied by Time-Resolved X-ray Liquidography (Solution Scattering). *ChemPhysChem* **2009**, *10*, 1958–1980.

(3) Ihee, H.; Wulff, M.; Kim, J.; Adachi, S. Ultrafast X-ray Scattering: Structural Dynamics from Diatomic to Protein Molecules. *Int. Rev. Phys. Chem.* **2010**, *29*, 453–520.

(4) Ihee, H.; Lorenc, M.; Kim, T. K.; Kong, Q. Y.; Cammarata, M.; Lee, J. H.; Bratos, S.; Wulff, M. Ultrafast X-ray Diffraction of Transient Molecular Structures in Solution. *Science* **2005**, *309*, 1223–1227.

(5) Davidsson, J.; Poulsen, J.; Cammarata, M.; Georgiou, P.; Wouts, R.; Katona, G.; Jacobson, F.; Plech, A.; Wulff, M.; Nyman, G.; Neutze, R. Structural Determination of a Transient Isomer of CH_2I_2 by Picosecond X-ray Diffraction. *Phys. Rev. Lett.* **2005**, *94*, 245503.

(6) Plech, A.; Kotaidis, V.; Lorenc, M.; Boneberg, J. Femtosecond Laser Near-Field Ablation from Gold Nanoparticles. *Nat. Phys.* **2006**, *2*, 44–47.

(7) Kim, T. K.; Lorenc, M.; Lee, J. H.; Lo Russo, M.; Kim, J.; Cammarata, M.; Kong, Q.; Noel, S.; Plech, A.; Wulff, M.; Ihee, H. Spatiotemporal Reaction Kinetics of an Ultrafast Photoreaction Pathway Visualized by Time-Resolved Liquid X-ray Diffraction. *Proc. Natl. Acad. Sci. U.S.A.* **2006**, *103*, 9410–9415.

(8) Georgiou, P.; Vincent, J.; Andersson, M.; Wohri, A. B.; Gourdon, P.; Poulsen, J.; Davidsson, J.; Neutze, R. Picosecond Calorimetry: Time-Resolved X-ray Diffraction Studies of Liquid CH_2Cl_2. *J. Chem. Phys.* **2006**, *124*, 234507.

(9) Kotaidis, V.; Dahmen, C.; von Plessen, G.; Springer, F.; Plech, A. Excitation of Nanoscale Vapor Bubbles at the Surface of Gold Nanoparticles in Water. *J. Chem. Phys.* **2006**, *124*, 184702.

(10) Cammarata, M.; Levantino, M.; Schotte, F.; Anfinrud, P. A.; Ewald, F.; Choi, J.; Cupane, A.; Wulff, M.; Ihee, H. Tracking the Structural Dynamics of Proteins in Solution Using Time-Resolved Wide-Angle X-ray Scattering. *Nat. Methods* **2008**, *5*, 881–886.

(11) Lee, J. H.; Kim, J.; Cammarata, M.; Kong, Q.; Kim, K. H.; Choi, J.; Kim, T. K.; Wulff, M.; Ihee, H. Transient X-ray Diffraction Reveals Global and Major Reaction Pathways for the Photolysis of Iodoform in Solution. *Angew. Chem., Int. Ed.* **2008**, *47*, 1047–1050.

(12) Lee, J. H.; Kim, T. K.; Kim, J.; Kong, Q.; Cammarata, M.; Lorenc, M.; Wulff, M.; Ihee, H. Capturing Transient Structures in the Elimination Reaction of Haloalkane in Solution by Transient X-ray Diffraction. *J. Am. Chem. Soc.* **2008**, *130*, 5834–5835.

(13) Plech, A.; Kotaidis, V.; Siems, A.; Sztucki, M. Kinetics of the X-ray Induced Gold Nanoparticle Synthesis. *Phys. Chem. Chem. Phys.* **2008**, *10*, 3888–3894.

(14) Christensen, M.; Haldrup, K.; Bechgaard, K.; Feidenhans'l, R.; Kong, Q. Y.; Cammarata, M.; Lo Russo, M.; Wulff, M.; Harrit, N.; Nielsen, M. M. Time-Resolved X-ray Scattering of an Electronically Excited State in Solution. Structure of the $^3A_{2u}$ State of Tetrakis-μ-pyrophosphitodiplatinate(II). *J. Am. Chem. Soc.* **2009**, *131*, 502–508.

(15) Haldrup, K.; Christensen, M.; Cammarata, M.; Kong, Q.; Wulff, M.; Mariager, S. O.; Bechgaard, K.; Feidenhans'l, R.; Harrit, N.; Nielsen, M. M. Structural Tracking of a Bimolecular Reaction in Solution by Time-Resolved X-Ray Scattering. *Angew. Chem., Int. Ed.* **2009**, *48*, 4180–4184.

(16) Szabo, A. Theory of Fluorescence Depolarization in Macromolecules and Membranes. *J. Chem. Phys.* **1984**, *81*, 150–167.

(17) Rothschild, W. G. *Dynamics of Molecular Liquids*; Wiley: New York, 1984.

(18) Fleming, G. R. *Chemical Applications of Ultrafast Spectroscopy*; Oxford University Press: New York, 1986.

(19) Fourkas, J. T.; Trebino, R.; Fayer, M. D. The Grating Decomposition Method: A New Approach for Understanding Polarization-Selective Transient Grating Experiments. I. Theory. *J. Chem. Phys.* **1992**, *97*, 69–77.

(20) Tokmakoff, A. Orientational Correlation Functions and Polarization Selectivity for Nonlinear Spectroscopy of Isotropic Media. I. Third Order. *J. Chem. Phys.* **1996**, *105*, 1–12.

(21) Baskin, J. S.; Zewail, A. H. Femtosecond Real-Time Probing of Reactions. 15. Time-Dependent Coherent Alignment. *J. Phys. Chem.* **1994**, *98*, 3337–3351.

(22) Brown, E. J.; Pastirk, I.; Dantus, M. Ultrafast Rotational Anisotropy Measurements: Unidirectional Detection. *J. Phys. Chem. A* **1999**, *103*, 2912–2916.

(23) Kim, Y. R.; Lee, M.; Thorne, J. R. G.; Hochstrasser, R. M. Picosecond Reorientations of the Transition Dipoles in Polysilanes Using Fluorescence Anisotropy. *Chem. Phys. Lett.* **1988**, *145*, 75–80.

(24) Kim, J.; Park, S.; Scherer, N. F. Ultrafast Dynamics of Polarons in Conductive Polyaniline: Comparison of Primary and Secondary Doped Forms. *J. Phys. Chem. B* **2008**, *112*, 15576–15587.

(25) Jonas, D. M.; Lang, M. J.; Nagasawa, Y.; Joo, T.; Fleming, G. R. Pump−Probe Polarization Anisotropy Study of Femtosecond Energy Transfer within the Photosynthetic Reaction Center of *Rhodobacter Sphaeroides* R26. *J. Phys. Chem.* **1996**, *100*, 12660–12673.

(26) Mirkovic, T.; Doust, A. B.; Kim, J.; Wilk, K. E.; Curutchet, C.; Mennucci, B.; Cammi, R.; Curmi, P. M. G.; Scholes, G. D. Ultrafast Light Harvesting Dynamics in the Cryptophyte Phycocyanin 645. *Photochem. Photobiol. Sci.* **2007**, *6*, 964–975.

(27) Woutersen, S.; Bakker, H. J. Resonant Intermolecular Transfer of Vibrational Energy in Liquid Water. *Nature* **1999**, *402*, 507–509.

(28) Kraemer, D.; Cowan, M. L.; Paarmann, A.; Huse, N.; Nibbering, E. T. J.; Elsaesser, T.; Miller, R. J. D. Temperature Dependence of the Two-Dimensional Infrared Spectrum of Liquid H_2O. *Proc. Natl. Acad. Sci. U.S.A.* **2008**, *105*, 437–442.

(29) Ji, M.; Odelius, M.; Gaffney, K. J. Large Angular Jump Mechanism Observed for Hydrogen Bond Exchange in Aqueous Perchlorate Solution. *Science* **2010**, *328*, 1003–1005.

(30) Hoshina, K.; Yamanouchi, K.; Ohshima, T.; Ose, Y.; Todokoro, H. Direct Observation of Molecular Alignment in An Intense Laser Field by Pulsed Gas Electron Diffraction I: Observation of Anisotropic Diffraction Image. *Chem. Phys. Lett.* **2002**, *353*, 27–32.

(31) Baskin, J. S.; Zewail, A. H. Ultrafast Electron Diffraction: Oriented Molecular Structures in Space and Time. *ChemPhysChem* **2005**, *6*, 2261–2276.

(32) Baskin, J. S.; Zewail, A. H. Oriented Ensembles in Ultrafast Electron Diffraction. *ChemPhysChem* **2006**, *7*, 1562–1574.

(33) Reckenthaeler, P.; Centurion, M.; Fuss, W.; Trushin, S. A.; Krausz, F.; Fill, E. E. Time-Resolved Electron Diffraction from Selectively Aligned Molecules. *Phys. Rev. Lett.* **2009**, *102*, 213001.

(34) Kim, J.; Kim, K. H.; Lee, J. H.; Ihee, H. Ultrafast X-ray Diffraction in Liquid, Solution, and Gas: Present Status and Future Prospects. *Acta Crystallogr., Sect. A* **2010**, *66*, 270–280.

(35) Wang, D.; Kreutzer, U.; Chung, Y.; Jue, T. Myoglobin and Hemoglobin Rotational Diffusion in the Cell. *Biophys. J.* **1997**, *73*, 2764–2770.

(36) Wilbur, D. J.; Norton, R. S.; Clouse, A. O.; Addleman, R.; Allerhand, A. Determination of Rotational Correlation Times of Proteins in Solution from Carbon-13 Spin-Lattice Relaxation Measurements. Effect of Magnetic Field Strength and Anisotropic Rotation. *J. Am. Chem. Soc.* **1976**, *98*, 8250–8254.

(37) Ansari, A.; Jones, C. M.; Henry, E. R.; Hofrichter, J.; Eaton, W. A. Photoselection in Polarized Photolysis Experiments on Heme Proteins. *Biophys. J.* **1993**, *64*, 852–868.

(38) Richard, L.; Genberg, L.; Deak, J.; Chiu, H.-L.; Miller, R. J. D. Picosecond Phase Grating Spectroscopy of Hemoglobin and Myoglobin: Energetics and Dynamics of Global Protein Motion. *Biochemistry* **1992**, *31*, 10703–10715.

(39) Franzen, S.; Bohn, B.; Poyart, C.; Martin, J. L. Evidence for Sub-Picosecond Heme Doming in Hemoglobin and Myoglobin: A Time-Resolved Resonance Raman Comparison of Carbonmonoxy and Deoxy Species. *Biochemistry* **1995**, *34*, 1224–1237.

(40) Ahn, S.; Kim, K. H.; Kim, Y.; Kim, J.; Ihee, H. Protein Tertiary Structural Changes Visualized by Time-Resolved X-ray Solution Scattering. *J. Phys. Chem. B* **2009**, *113*, 13131–13133.

(41) Kim, K. H.; Oang, K. Y.; Kim, J.; Lee, J. H.; Kim, Y.; Ihee, H. Direct Observation of Myoglobin Structural Dynamics from 100 ps to

1 Microseond with Picosecond X-ray Solution Scattering. *Chem. Commun.* **2011**, *47*, 289–291.

(42) Cho, H. S.; Dashdorj, N.; Schotte, F.; Graber, T.; Henning, R.; Anfinrud, P. A. Protein Structural Dynamics in Solution Unveiled via 100-ps Time-Resolved X-ray Scattering. *Proc. Natl. Acad. Sci. U.S.A.* **2010**, *107*, 7281–7286.